HYBRID CURRENT CONTROL TECHNIQUE COMBINATION OF TIME DOMAIN AND FREQUENCY DOMAIN CURRENT CONTROLLER

[1] Nazma begum, [2] Chandrashekara Seregara
[1] M.tech student, [2] Asst. Professor
[1] Dept of Power Electronics, PDA engineering college, Kalaburagi, Karnataka,India.

ABSTRACT

This paper proposes an advanced current controller for grid-connected bi-directional AC/DC converters used for Energy Storage Systems (ESSs). The proposed control scheme is designed to combine both the time-domain and frequency-domain properties to achieve better transient and steady-state performance. The power electronic loads with a non-linear relationship between voltages and currents have led to increasing current and voltage distortion in distribution systems. The Hybrid Partitioned Frequency-Time domain approach is done using the solar and fuel cell. And across the battery just connecting one electric vehicle, when it is in idle mode battery will provide the charge to grid under, and when it is in running mode the battery will be disconnected. And while it is running and suddenly stopping at the time we can provide regenerative braking. When the time slot of 0.4s, the vehicle is in idle mode and the battery is connected to the system and after 0.4s, the vehicle starts running and battery will be disconnected from grid. Torque stored in the winding or some machine will be fed back to battery.

KEY WORDS

Energy Storage Systems, Smart Grid, Micro/Nano-Grid, Hybrid Renewable Energy Systems, AC/DC Converter, Bi-Directional Converter, Grid-Connected Converter, Slow Manifold, Fast Manifold, Nonlinear Control, Adaptive Control.

INTRODUCTION

Recent advancements in the application of digital control to power electronics has given considerable momentum to global energy management [1]-[2]. These developments are turning smart grids into a viable solution for future energy management. The efficient energy management of various distributed energy sources is a promising solution to the future energy crisis. The intelligent energy management of the aforementioned components is the key to the successful implementation of a smart grid.

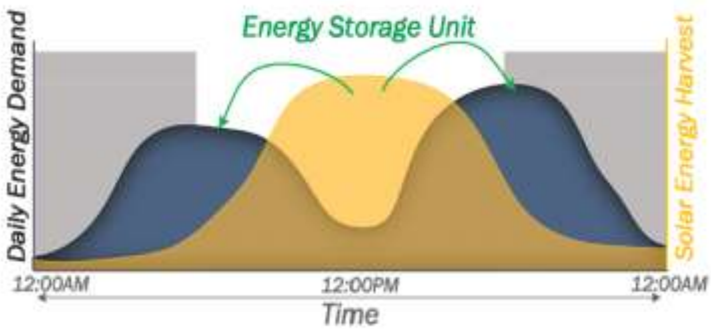

Fig. 1: Energy storage units can complement solar energy by storing and releasing energy when needed for residential applications.

In particular, the integration of roof-top solar panels and energy storage units is well-suited towards residential applications. The required energy is needed mostly during mornings and evenings. However, solar energy can be harvested only during the daytime (especially in the afternoon). This mismatch reinforces the need for local energy storage units. Local energy storage units can effectively store and release energy as required. Fig.2 shows a daily distribution of the energy demand for a typical household. According to this figure, the energy storage unit is able to store energy during the day when the harvested solar energy is at its peak and then release the energy in the morning and the evenings when there is a higher energy demand. Bi-directional grid-connected AC/DC converters are a key component used for interfacing energy storage units to the utility grid, and they are essential for the integration of energy storage into future smart grids. An important feature of grid-connected DC distribution system is the ability to inject or suck power from the grid based on the generation and loading conditions. In order to do that, a controlled AC-DC/DC-AC converter that allows bidirectional power flow has been used. This controlled converter is responsible for controlling the amount of power flow between the AC and the DC grid.

Tracking a sinusoidal reference is challenging, as discussed in [4]-[5]. Conventionally, a fast Proportional Integral (PI) controller has widely been used in this application[6]-[9]. PI-controllers can handle tracking a DC reference due to their high gain at a frequency of zero. Since the grid frequency is relatively low, PI-controllers can produce a reasonably high gain at the grid frequency as well. Thus, a PI-controller with a high bandwidth can technically be used for this application. However, very high gain PI-controllers is marginally stable and still introduces some phase delay while tracking a sinusoidal signal. In order to solve this issue, Proportional-Resonant (PR) controllers have been introduced[10]-[11]. For three-phase systems, synchronous frame PI control with voltage feedforward can be used, but it usually requires multiple frame transformations, and can be difficult to implement using a low-cost fixed-point digital signal processor (DSP). Overcoming the computational burden and still achieving virtually similar frequency response characteristics as a synchronous frame PI controller, develops the P+resonant (PR) controller for reference tracking in the stationary frame. Interestingly, the same control structure can also be used for the precise control of a single-phase converter. PR controllers are equivalent to conventional PI controller implemented in two synchronous rotating frames (positive sequence and negative sequence) and hence able to track sinusoidal references with variable frequency of both positive and negative sequences with zero steady state error. The transfer function of PR controller can be derived by using internal control model with modified state transformation or frequency domain approach. In brief, the basic functionality of the PR controller is to introduce an infinite gain at a selected resonant frequency for eliminating steady state error at that frequency, and is therefore conceptually similar to an integrator whose infinite DC gain forces the DC steady-state error to zero.

PROPOSED CLOSED LOOP CURRENT CONTROLLER FOR AC/DC CONVERTER

The control system for the AC/DC converter is usually designed in the frequency-domain without considering the dynamics of the converter in the time-domain. Normally, a PR-controller tuned to the fundamental component as well as a harmonic compensator tuned to the harmonics is used to control the AC/DC converter. Although this approach is very easy to design, it carries the difficulties explained in the previous section.

This paper presents a current control technique, which combines the controller design in the time-domain as well as the frequency-domain. Thus, the proposed control approach can offer a much better transient and steady-state performance compared to the conventional control techniques. In the time domain, the controller is developed using the converter dynamics, and in the frequency-domain the gain of the compensator is adjusted such that there is a very high gain at the line frequency as well as the harmonics.

A. Time domain current controller

In this section, the design of the current controller in the time-domain is described. This design is performed using the dynamics of the AC/DC converter. The dynamics of the converter in the time-domain is given by:

$$\frac{di_g}{dt} = \frac{1}{L_g}v_g - \frac{1}{L_g}v_{BUS}u(t) \quad (1)$$

$$\frac{dv_{BUS}}{dt} = \frac{1}{C_{BUS}}i_g u(t) - \frac{1}{C_{BUS}R_e}v_{BUS} \quad (2)$$

Where u(t) = 2d(t) − 1 and d(t) is the duty ratio of the bridge output voltage and Re is the load seen from the output capacitor.

Eqs. (1)-(2) describe the nonlinear dynamics due to the coupling between the control input, u and the state variables, i_g and v_{BUS}. In order to design the closed-loop control system for these dynamics, the singular perturbation control theory can be used [15]. Since the dynamics of the DC-bus voltage, v_{BUS} are much slower than those of the grid current i_g, the dynamics of the system can be divided into two subsystems. The first subsystem represents the fast dynamics and includes the state variable with a much higher rate of change, namely i_g, and the second subsystem represents the slow dynamics, which includes the slow state variable, namely v_{BUS}. This theory allows a typical nonlinear system to be broken down into subsystems with different time scales. Since the internal control loop is much faster than the external control loop, this theory can be applied to the closed-loop control system.

$$\frac{dv_{BUS}}{dt} = f(v_{BUS}, i_g, t) \quad (3)$$

$$\mu\frac{di_g}{dt} = g(v_{BUS}, i_g, t) \quad (4)$$

the singular limit, $\mu = 0$, is used to obtain the following system,

$$\frac{dv_{BUS}}{dt} = f(v_{BUS}, i_g, t) \quad (5)$$

$$i_g = \emptyset(v_{BUS}, t) \quad (6)$$

Where the second of these equations is the solution of $g(v_{BUS}, i_g, t)$. Eqs.(5)-(6) are called a degenerate system. When μ converges to zero, the solution of the system (3)-(4) tends to the solution of the degenerate system if $i_g = \emptyset(v_{BUS}, t)$ is a stable root of the adjoined system $\mu\frac{di_g}{dt} = g(v_{BUS}, i_g, t)$.

In the AC/DC converter, the slow dynamics are described by (2) and the fast dynamics are described by (1). Therefore, if the compensator designed for the fast dynamics is stable then the conditions of Tikhonov's theorem are satisfied, and in turn the dynamics can be treated separately. In order to design a stable compensator, the grid current tracking error is defined by:

$$e_{i,t} = i_{g,ref} - i_g \quad (7)$$

The compensator must render this error zero while maintaining the stability of the closed-loop control system. The following energy function is defined in order to design the current compensator in the time domain:

$$V_i = \frac{1}{2} e_{i,t}^2 \quad (8)$$

The derivative of the energy function is given by:

$$V_i = \dot{e}_{i,t} e_{i,t} = e_{i,t}\left(\frac{dig,ref}{dt} - \frac{1}{L_g} v_g + \frac{1}{L_g} \bar{v}_{BUS}\, u(t)\right) \quad (9)$$

It should be noted that v_{BUS} can be considered constant to design the compensator according to Tikhonov's theorem. Thus, it is shown as $\bar{v}_{BUS}$ in (9). According to (9), the time-domain compensator is designed as:

$$u(t) = \frac{1}{\bar{v}_{BUS}}\left(v_g - L_g \frac{dig,ref}{dt} - k e_{i,t}\right) \quad (10)$$

The control law given by (10) guarantees the asymptotic convergence of the current error to zero. In the digital implementation, the time-domain controller is given by:

$$u_t(n) = \frac{1}{\bar{v}_{BUS}(n)}\left(v_g - L_g \frac{i_{g,ref}(n) - i_{g,ref(n-1)}}{T_s}\right) \quad (11)$$

The time-domain controller is designed based on the dynamics of the system. Therefore, it has more capability to improve the transient response compared to the PR-controller, which does not act with awareness of the system dynamics.

B. Frequency-Domain Current Controller

In order to track a sinusoidal reference, the current controller should have a very high gain at the frequency of the sinusoidal signal according to the Internal Model Principle (IMP) [14]. The coefficients of the current control scheme are produced by the update laws. The update laws use the value of the current error to make adjustments to the nominal coefficients such that the steady-state error is rendered zero. The update laws for the current control scheme in this paper are given by:

$$\dot{\hat{a}} = \gamma_a e_i \sin(\omega_l t) \quad (12)$$

$$\dot{\hat{b}} = \gamma_b e_i \sin(\omega_l t) \quad (13)$$

Therefore, by using the bilinear transformation, the proposed frequency-domain control law in the discrete domain is given by:

$u_f(n)$ = (n)−(n−2)+uf (n−1)^a(n)−uf (n−2)

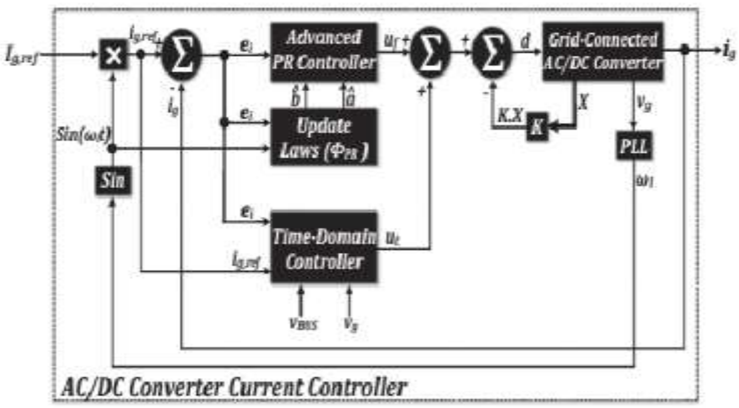

Fig. 2: Combined time-domain and frequency-domain closed loop current control system.

Fig. 2, the block diagram of the proposed closed-loop control system is presented. This figure shows that the current controller combines the time-domain controller and the frequency-domain controller in order to achieve optimal transient and steady-state performance. The frequency-domain controller includes the advanced PR-controller, which provides a high gain at the line frequency. The advanced PR-controller does not require an extra PI-controller, which is usually superimposed onto conventional PR-controllers in order to eliminate the DC component of then error signal. This is due to the fact that when the coefficient $\hat{a}(n)$ approaches 2, the advanced PR-controller is equivalent to a PI-controller. Also, if the sampling frequency is high enough, the proposed advanced PR-controller eliminates the need for a harmonic compensator. If the sampling frequency is high the a-coefficients of the PR-controllers for the fundamental and harmonics are very close and the adaptive scheme covers the entire bandwidth including the harmonics.

SIMULATION FOR THE PROPOSED SYSTEM

Fig.3 shows the simulation diagram for the proposed system using MATLAB Simulink R2014a version by using different Sim power system components.

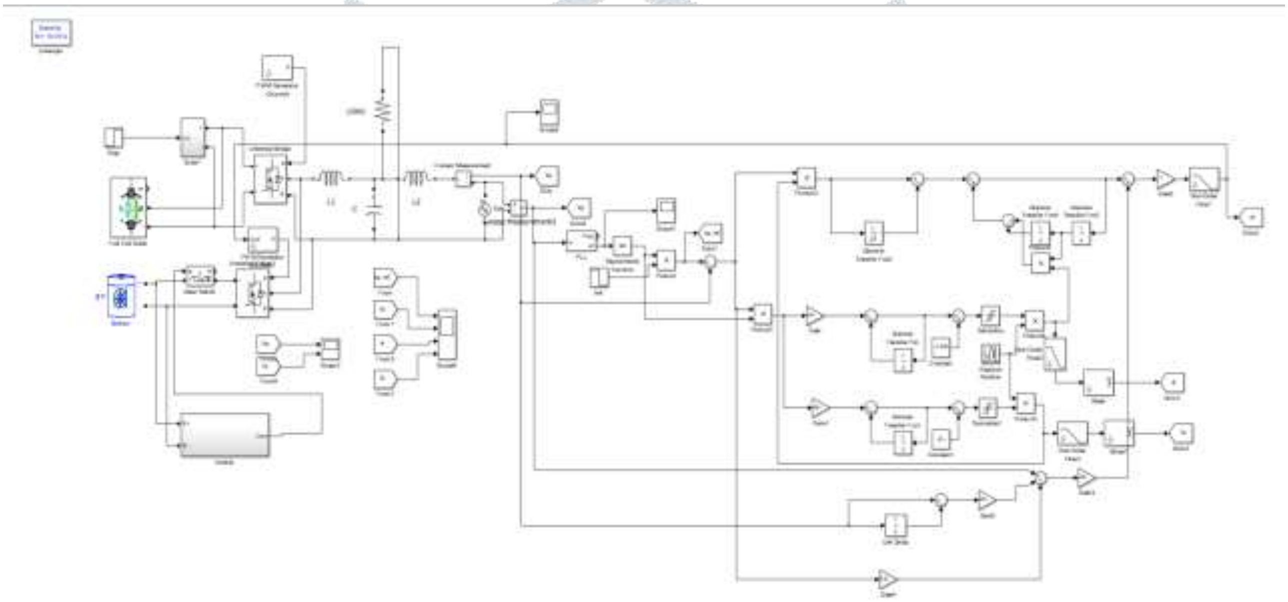

Fig.3: Proposed Simulation diagram

SIMULATION RESULTS

Simulation model is tested and fabricated using MATLAB R2014a software. And the snap charts of input and output voltages are taken. These waveforms are shown in following figures. And the harmonics for different frequencies are shown in Table-1.

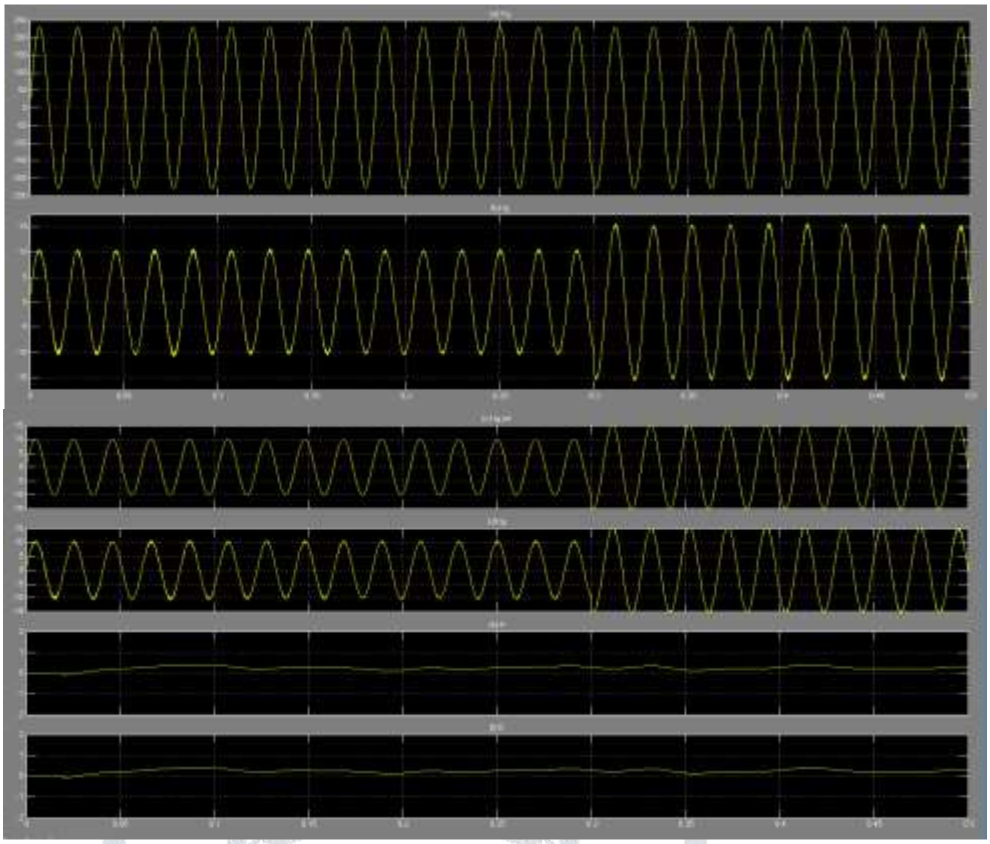

Fig.4: Transient performance of the proposed closed-loop current controller for a positive step in the current reference signal .

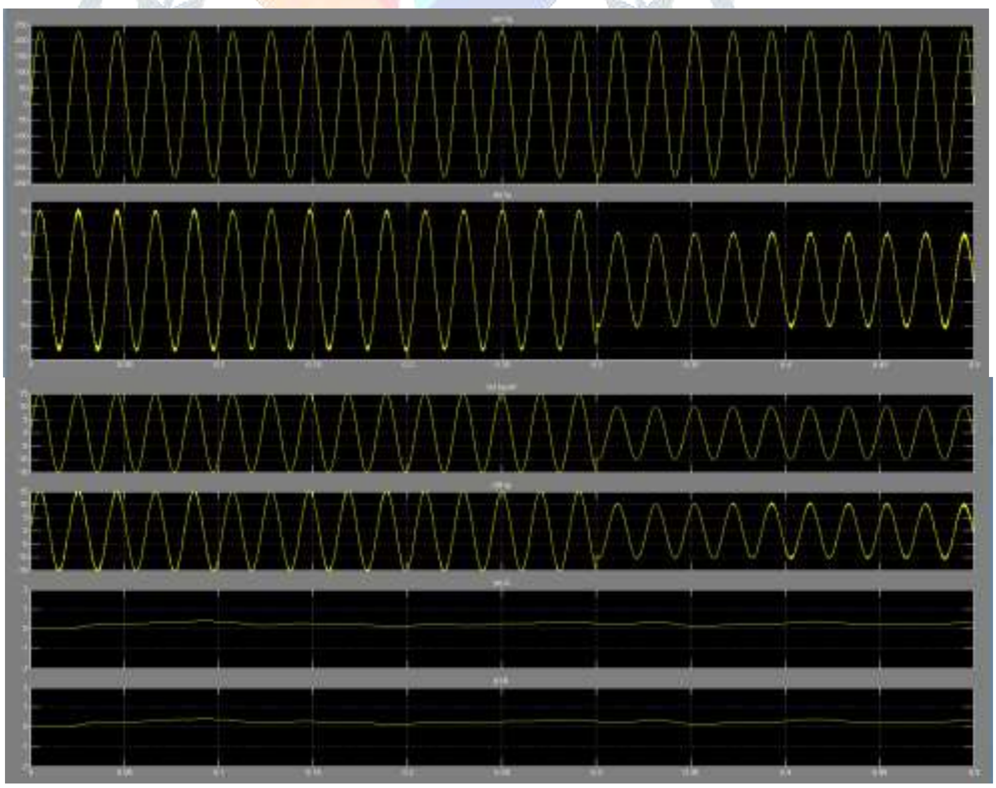

Fig.5: Transient response of the proposed closed-loop current controller for a negative step in the current reference signal.

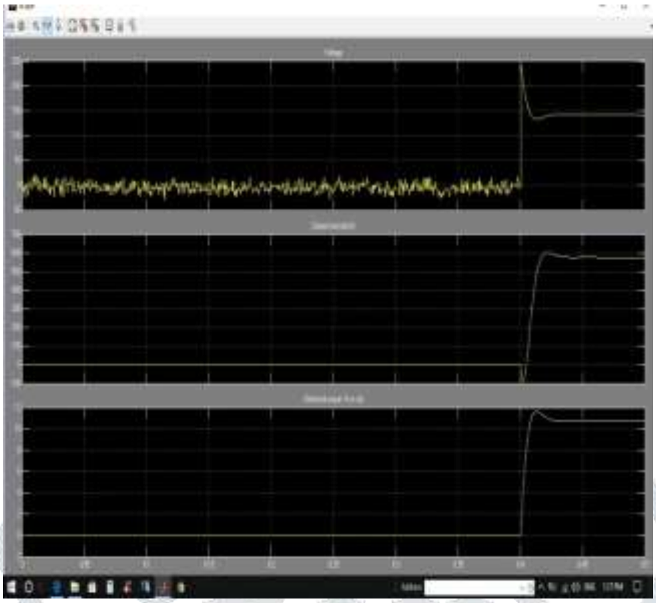

Fig.6: Transient performance of the electric vehicle voltage, speed and torque

Table 1
HARMONICS FOR THE DIFFERENT FREQUENCY

Harmonics	For 49Hz	For 50Hz
3rd – Harmonic	0.84%	0.10%
5th – Harmonic	0.43%	0.06%
7th – Harmonic	0.29%	0.04%
9th – Harmonic	0.22%	0.03%

CONCLUSIONS

An advanced PR-controller is used as a current controller for a grid-connected AC/DC converter. The advanced PR-controller is designing in both the time-domain and the frequency-domain. The frequency-domain controller adaptively changes the co-efficient of the PR-controller based on the current error to steer the error towards zero. The time-domain controller operates by minimizing the derivative of a defined energy function. The advanced PR-controller is able to overcome the various challenges faced by the conventional PR-controller, which cause steady-state errors in the tracking of the sinusoidal reference for the grid current and impaired transient performance. Across the battery one electric vehicle is connected. When the time slot of 0.4s, the vehicle is in idle mode and the battery is connected to the system and after 0.4s, the vehicle starts running and battery will be disconnected from grid. Torque stored in the winding or some machine will be fed back to battery.

REFERENCES

1. Divan, D.; Moghe, R.; Prasai, A., ”Power Electronics at the Grid Edge : The key to unlocking value from the smart grid,” Power Electronics Magazine, IEEE , vol.1, no.4, pp.16,22, Dec. 2014.
2. Popovic-Gerber, J.; Oliver, J.A.; Cordero, N.; Harder, T.; Cobos, J.A.; Hayes, M.; O’Mathuna, S.C.; Prem, E., ”Power Electronics Enabling Efficient Energy Usage: Energy Savings Potential and Technological Challenges,” Power Electronics, IEEE Transactions on , vol.27, no.5, pp.2338,2353, May 2012.
3. Eren, S.; Pahlevani, M.; Bakhshai, A.; Jain, P., ”An Adaptive Droop DC-Bus Voltage Controller for a Grid-Connected Voltage Source Inverter With LCL Filter,” Power Electronics, IEEE Transactions on , vol.30, no.2, pp.547,560, Feb. 2015.
4. Weizhou Su; Qiu, L.; Jie Chen, ”On performance limitation in tracking a sinusoid,” Automatic Control, IEEE Transactions on , vol.51, no.8, pp.1320,1325, Aug. 2006.
5. Fukuda, S.; Yoda, T., ”A novel current-tracking method for active filters based on a sinusoidal internal model [for PWM invertors],” Industry Applications, IEEE Transactions on , vol.37, no.3, pp.888,895, May/Jun 2001.
6. Erika Twining; Holmes, D.G., ”Grid current regulation of a three-phase voltage source inverter with an LCL input filter,” Power Electronics, IEEE Transactions on , vol.18, no.3, pp.888,895, May 2003.
7. Blaabjerg, F.; Teodorescu, R.; Liserre, M.; Timbus, A.V., ”Overview of Control and Grid Synchronization for Distributed Power Generation Systems,” Industrial Electronics, IEEE Transactions on , vol.53, no.5, pp.1398,1409, Oct. 2006.
8. Espi Huerta, J.M.; Castello-Moreno, J.; Fischer, J.R.; Garcia-Gil, R., ”A Synchronous Reference Frame Robust Predictive Current Control for Three-Phase Grid-Connected Inverters,” Industrial Electronics, IEEE Transactions on , vol.57, no.3, pp.954,962, March 2010.
9. Adda, R.; Ray, O.; Mishra, S.K.; Joshi, A., ”Synchronous-ReferenceFrame-Based Control of Switched Boost Inverter for Standalone DC Nanogrid Applications,” Power Electronics, IEEE Transactions on , vol.28, no.3, pp.1219,1233, March 2013.
10. X. Yuan, W. Merk, H. Stemmler, and J. Allmeling, Stationary-frame generalized integrators for current control of active power filters with zero steady-state error for current harmonics of concern under unbalanced and distorted operating conditions, IEEE Trans. Ind. Appl., vol. 38, no. 2, pp. 523532, Mar./Apr. 2002.
11. D. Zmood and D. G. Holmes, Stationary frame current regulation of PWM inverters with zero steady-state error, IEEE Trans. Power Electron., vol. 18, no. 3, pp. 814822, May 2003.
12. Li, Bin; Zhang, Ming; Huang, Long; Hang, Lijun; Tolbert, Leon M., ”A robust multi-resonant PR regulator for three-phase grid-connected VSI using direct pole placement design strategy,” Applied Power Electronics Conference and Exposition (APEC), 2013 Twenty-Eighth Annual IEEE , vol., no., pp.960,966, 17-21 March 2013.
13. F. Liu, Y. Zhou, S. Duan, J. Yin, B. Liu, and F. Liu, Parameter design of a two-current-loop controller used in a grid-connected inverter system with LCL filter, IEEE Trans. Ind. Electron., vol. 56, no. 11, pp. 44834491, Nov. 2009.
14. B. Francis and W. Wonham, The internal model principle of control theory, Automatica, vol. 12, no. 5, pp. 457465, Sep. 1976.
15. W. Longke, W. J. Book, and J. D. Huggins, Application of singular perturbation theory to hydraulic pump controlled systems, IEEE/ASME Trans. Mechatronics, vol. 17, no. 2, pp. 251259, Apr. 2012.